DINAME 2023 - Proceedings of the XIX International Symposium on Dynamic Problems of Mechanics,
A.S. De Paula, A.T. Fabro and M.R. Machado (Editors), ABCM.
Pirenópolis, Go, Brazil, February 26th to March 3rd, 2023

Bolted joints parameter estimation using Bayesian Inference

Vitória Duarte [1] **and Marcela Rodrigues Machado.**

[1] Department of Mechanical Engineering, Universidade of Brasília. Campus Universitário Darcy Ribeiro, Faculdade de Tecnologia - Asa Norte, Brasília - DF, 70910-900, Brazil, vcarolinaduarte@gmail.com

Abstract: Physical data are typically used to calibrate numerical models using forward or backward bias methods. In mechanical vibration, an one application of the inverse problem is when data such as displacements or frequency spectrum are obtained with precise sensors in a known range of applications. The complementary conditions are known - controlled experiment - and the desired properties are desired, e.g., equivalent stiffness, viscous dissipation coefficient, and natural frequency. Numerical modeling and estimation of the parameters can be challenging for more complex systems such as bolted joints. In this This work, a bolted beam system was modeled using the spectral element method and calibrated with driven data from the system's driven data. Bolted stiffness values (k_v and k_t) were estimated using Bayesian inference combined with the Markov-Chain Monte Carlo-Metropolis Hastings (MCMC-MH) algorithm. The results show good agreement between the Digital Twin and the physical unit.

Keywords: Spectral Element Method, Bolted structure, Markov-Chain Monte Carlo, UQLab, Digital Twin

INTRODUCTION

Structures and machines are built of connected components aiming the assemble and disassemble during an operation. Therefore, bolts are mechanical components that provide sufficient joint force to withstand external vibration, dynamic loads, or thermal fluctuations without yielding. A tightened bolt uses its elastic properties, modeled as a spring that changes its rigidity value when the torque is applied.

Several researchers have worked on modeling bolted joints. The finite element method (FEM) is one of the most numerical methods used (Oldfield, 2003, Knight, 2008, Zeng, 2011) due to its accurate and efficient representation. Kim *et al*. (2007) performed numerical simulations using the implicit FEM software package ANSYS for the pre-stress effect and contact behavior in the bolted joint of a marine diesel engine. Alfattani *et al*. (2020) describes the structural analysis of a preloaded bolted joint performed in the ANSYS software. Their parametric studies were conducted using elastic, high-strain, and nonlinear finite element analyses to determine the influence of various factors on the response. These factors included bolt preload, contact areas, boundary conditions, and length of the connecting segment. Soon and Kim (2007) used the same software to study the structural behavior of shear joints bolted with thin-walled stainless steel plates. Digital Twin (*DT*) has gained interest in recent years in both academia and industry because of its ability to create a numerical model with high accuracy for the real system. These physical data are used to calibrate the numerical model, for which one can use different techniques in direct or inverse bias (Wagg *et al.*, 2020).

There are many examples when the system is discrete and with a certain degree of freedom, but when looking for models such as beams and bars, that is, more complex systems such as bolted joints, one realizes that they are not always applied (Castello and Kaipio, 2019). As presented by Lee (2009), it is necessary to resort to numerical methods to search for approximate solutions when it is impossible to find them analytically, a typical case of partial differential equations, which govern the problems of dynamic vibrations in continuous systems. As Lee and Lee (1996), the Spectral Element Method (SEM) is applied to beams and bars - continuous systems - subjected to distributed dynamic forces because, in this method, the distributed equivalent spectral nodal forces can represent dynamic forces. Its techniques are based on the boundaries between computer simulation engineering, applied mathematics, statistics, and probability theory.

Many studies have focused primarily on estimating contact stress and bolt preload. It is necessary to evaluate the dynamic behavior of the bolted joint in service to avoid failure due to resonance. This work performs the Digital Twin calculation of beams connected with three bolted joints. The connected structure is modelled using the spectral element method, and the model is calibrated using data-driven obtained from Teloli *et al*. (2021) and Teloli *et al* (2021). Identification of the preload of the bolts, reflected in the stiffness, is estimated using Bayesian inference and Markov-Chain Monte Carlo Metropolis Hastings Algorithm.

SPECTRAL ELEMENT METHOD

The SEM was first proposed by Narayanan and Beskos (1978), further improved and named SEM by Doyle (1997) and Lee (2009). The SEM consists of the exact displacement of the wave equation of the analytical solution in the frequency domain. It is equivalent to an infinite number of finite elements. This characteristic and the spectral domain make SEM more suitable to solve the crack problem. The advantage of SEM is the reduced number of elements required to model the system as compared to other computational methods. SEM is similar in style to the FEM, it is written in

the frequency domain, and the element interpolation function is the exact analytical solution of the differential equation. These futures allows a no mesh element requirement associated with high accuracy in solve structural dynamic problems. The number of elements required for a spectral model will coincide with the number of discontinuities of the structure. Another significant advantage of using SEM is the throw-off element that consists of conduct to propagate energy out of the system, it works as an an-echoic termination dissipating the remaining energy in the system.

Beam spectral element

The beam is assumed as slender with transversal and rotational nodal displacement, shear and momentum nodal forces. By neglecting shear deformations, the differential equation of movement in its spectral form can be written as

$$\frac{d^4\hat{v}}{dx^4} - k^4\hat{v} = F, \tag{1}$$

with the homogeneous solution given by

$$\hat{v}(x,\omega) = a_1 e^{-ikx} + a_2 e^{-kx} + a_3 e^{-ik(L-x)} + a_4 e^{-k(L-x)}, \tag{2}$$

where

$$\mathbf{e}(x,\omega) = \begin{bmatrix} e^{-ikx} & e^{-kx} & e^{-ik(L-x)} & e^{-k(L-x)} \end{bmatrix}, \tag{3}$$

$$\mathbf{a} = \begin{bmatrix} a_1 & a_2 & a_3 & a_4 \end{bmatrix}^T, \tag{4}$$

for L being the beam length. The wavenumbers, k, k_1 and k_2 are given by

$$k^2 \equiv \sqrt{\frac{\omega^2 \rho A}{EI}}, \quad k_1 = \pm k, \quad k_2 = \pm ik, \tag{5}$$

where ω is the circular frequency, E is the Young's modulus, A is the cross-section area, ρ is the density, I is the inertia moment, and $i = \sqrt{-1}$. By using a complex Young's modulus, $E_c = E(1+i\eta)$, a internal structural damping is introduced where η is the hysteretic structural loss factor. Figure 1 illustrates a two nodes beam spectral element model with two degrees of freedom (DOF) per nodes. The nodal displacements are $\hat{v}$ and $\hat{\phi}$ and the nodal forces $\hat{V}$ and $\hat{M}$.

Figure 1: Spectral element of a two-node element with two displacement-related degrees of freedom and two forces per node.

The spectral nodal displacements and slopes of the finite beam element can be related to the displacement field as at node 1 ($x = 0$) and at node 2 ($x = L$)

$$d = \begin{Bmatrix} \hat{v_1} \\ \hat{\phi_1} \\ \hat{v_2} \\ \hat{\phi_2} \end{Bmatrix} = \begin{Bmatrix} \hat{v}(0) \\ \hat{v}\prime(0) \\ \hat{v}(L) \\ \hat{v}\prime(L) \end{Bmatrix} = \begin{Bmatrix} e(0,\omega) \\ e'(0,\omega) \\ e(L,\omega) \\ e'(L,\omega) \end{Bmatrix}, \tag{6}$$

where $\mathbf{a} = \mathbf{H_B}(\omega)^{-1}\mathbf{d}$, and

$$\mathbf{H_B}(\omega) = \begin{bmatrix} 1 & 1 & e^{-ikL} & e^{-kL} \\ -ik & -k & ike^{-ikL} & ke^{-kL} \\ e^{-ikL} & e^{-kL} & 1 & 1 \\ -ike^{-ikL} & -ke^{-kL} & ik & k \end{bmatrix}. \tag{7}$$

The frequency-dependent displacement within an element is interpolated from the nodal displacement vector, it is expressed as

$$\hat{v} = e(x,\omega)H_B^{-1}(\omega)\mathbf{d}. \tag{8}$$

Shear forces and bending moments defined for the beam is related to the defined forces and moments in a spectral nodal form as

$$f = \begin{Bmatrix} \hat{V}_1 \\ \hat{M}_1 \\ \hat{V}_2 \\ \hat{M}_2 \end{Bmatrix} = \begin{Bmatrix} -V(0) \\ -M(0) \\ V(L) \\ M(L) \end{Bmatrix} = \begin{Bmatrix} -\hat{v}(0)''' \\ -\hat{v}(0)'' \\ \hat{v}(L)''' \\ \hat{v}(L)'' \end{Bmatrix}. \tag{9}$$

where by applying boundary conditions it has,

$$f = EI \begin{Bmatrix} -ik^3 & k^3 & ie^{-ikL}k^3 & e^{-kL}k^3 \\ k^2 & -k^2 & e^{-ikL}k^2 & -e^{kL}k^2 \\ ie^{-ikL}k^3 & -e^{kL}k^3 & -ik^3 & k^3 \\ -e^{-ikL}k^2 & e^{-kL}k^2 & -k^2 & k^2 \end{Bmatrix} \mathbf{a} = G(\omega)\mathbf{a}. \tag{10}$$

By relating the nodal forces to the nodal displacement, one has

$$\mathbf{f} = \mathbf{G}(\omega)\mathbf{H}_B^{-1}(\omega)\mathbf{d} = \mathbf{S}(\omega)\mathbf{d} \tag{11}$$

where $\mathbf{S}(\omega) = \mathbf{G}(\omega)\mathbf{H}_B^{-1}(\omega)$ is the dynamic stiffness matrix of the Euler-Bernoulli beam spectral element.

Beam spectral element connected by bolt

The beam spectral element connected by bolt considered two beams coupled from one bolt is illustrated in Fig. 2(a), and the spectral bolt model, presented in (Lee, 2001, Machado *et al*.,2019) is equivalent of a lumped mass and a spring-system. The lumped mass has its mass m and the mass moment of inertia I, the spring-system consists of a linear stiffness (kv) and a torsional stiffness (kt), as shown in Fig.2 (b) the lumped mass and the spring-system are connected in series.

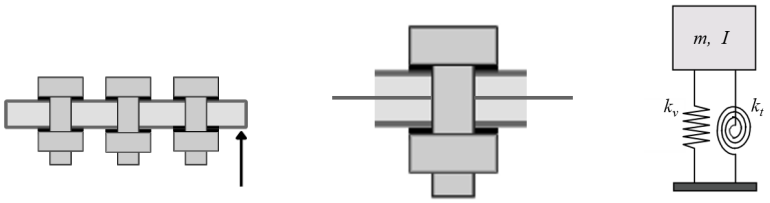

Figure 2: Representation: (a) Bolted beam example; (b) Physical bolted structure; (c) Spectral element model.

The symmetric dynamic spectral element matrix or the equivalent bolt-joint model, is expressed as (Lee, 2001),

$$\mathbf{S}_b(\omega) = \begin{bmatrix} k_v & 0 & -k_v & 0 \\ 0 & -k_t & 0 & k_t \\ -k_v & 0 & -m\omega^2 + k_v & 0 \\ 0 & k_t & 0 & -I\omega^2 - k_t \end{bmatrix}. \tag{12}$$

where ω is the circular frequency. One should note that the spectral element matrix $\mathbf{S}_b(\omega)$ includes of equivalent bolt-joint model parameters. Analogous to FEM, the SEM can be assembled to form a global structure matrix system.

Bayesian Inference

In the Bayesian approach, the inverse problem is reformulated into a search for information using statistical tools. The goal of Bayesian inference is to prove all available information about a problem using probability statements by Bayes' theorem, as shown in Fig. 3, from the observed data. Quantifying uncertainty through computer simulation is an inherently interdisciplinary method whose application has grown rapidly in recent decades.

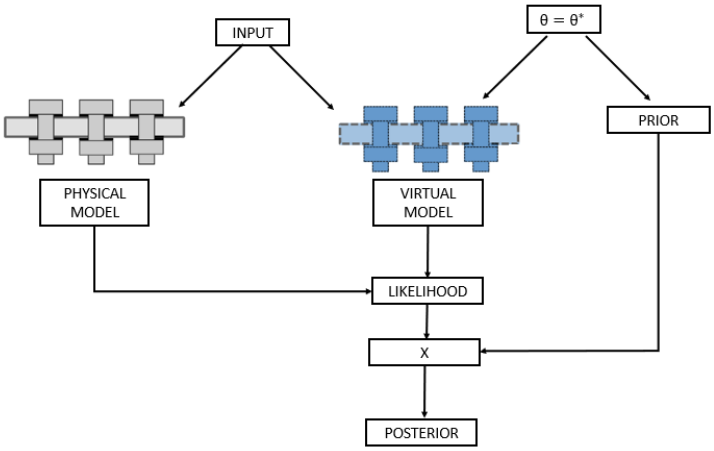

Figure 3: Schematic for the Bayesian paradigm in Bayesian Inference.

In general terms, it aims to identify the sources of uncertainty in each component of the simulation of physical quantities and the propagation of this uncertainty in the model responses. Such a formulation encompasses a range of approaches, including but not limited to structural reliability, sensitivity analysis, reliability-based design optimization, and Bayesian techniques for calibration and validation of computer models.

NUMERICAL RESULTS

Application of Bayesian inference using MCMC - MH with 20 chains and 1,000 iterations each, giving a total of 20,000 samples. To estimate the bolt structural parameters (k_v and k_t) we used the experimental dynamic response of the bolted beams, which the parameters are displayed in Table 1. The data-driven considered in the work are from the works of Teloli *et al*., (2021) and Teloli *et al*., (2021). The parameters to be derived must obey a log-normal distribution as oriented in the UQLab manual (Lataniotis, Marelli and Sudret, 2021), where the range is the standard deviation, which was assumed to be 10% of the reference values.

Table 1: Properties of the bolted jointed.

Parameter nominal	**Value**
Vertical stiffness (k_v)	4.980 10^5 N/m^2
Torsional stiffness (k_t)	4.1233 10^4 N/m^2
Modulus of elasticity (E)	7.3105 10^3 Pa
Specific density (ρ)	2790 kg/m^3
Preload (T)	80 N.m

Figure 4 shows the evolution of twenty Markov chains for each of one thousand iterations and their respective adjoint Kernel Density Graph (KDE). In Fig. 4, it can be seen that the generated MCMC chains have converged to the reference value of the parameters. Moreover, the KDE graph is well defined according to the assumed distribution, indicating convergence of the Markov chain. As described earlier, the initial information for the parameter of interest is a log-normal probability distribution. The UQLab toolbox also generates a report with the results, in which the percentage error is estimated, so the values in Tab. 2, and we have the following results:

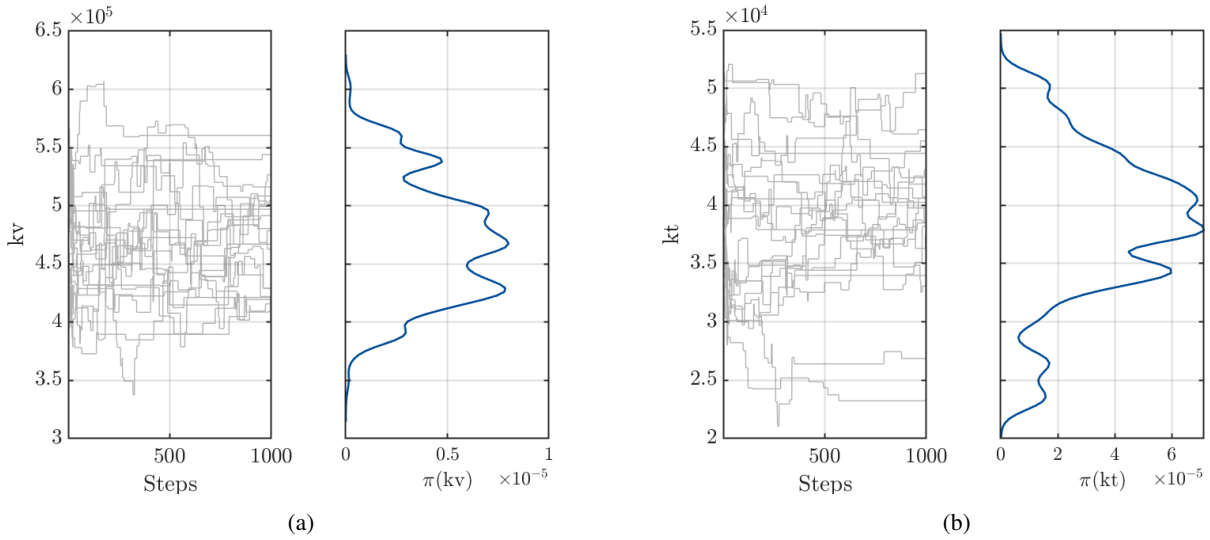

Figure 4: Trace and corresponding KDE plots during the MCMC-MH run of the estimated parameters (a) vertical stiffness and (b) torsional stiffness for preload of 80N.m.

Table 2: Nominal value, expected mean, the experimental error, and the relative percent error for the parameters.

γ_{ref}	γ_{est}	σ_{error}	**Error%**
$4.980\ 10^5$	$4.4988\ 10^5$	$1.027\ 10^{-8}$	9.66%
$4.1233\ 10^4$	$3.6990\ 10^4$	$1.027\ 10^{-8}$	10.29%

Table 3: The correlation matrix of the parameters for 80 N.m preload.

	(k_v)	(k_t)
(k_v)	1	0.012
(k_t)	0.012	1

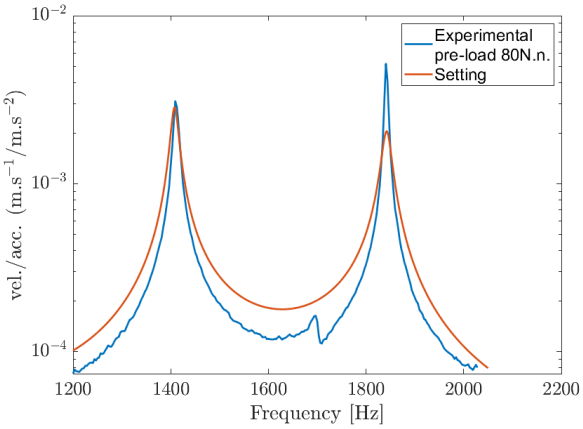

Figure 5: FRFs of the estimated parameters for each experimental data and the experimental data of the bolted joint.

The correlation matrix between the parameters is of 1.2% as shown in Table 3, it determines the percentage that one parameter relates to the other. The relative error was less than 11%, so the result can be considered accurate. Figure 5 shows the estimated FRFs for each data set along with the model and experimental FRFs. It is clear that not only a good data set but also the location where these data were collected should be considered in the analysis. The stochastic MCMC method was applied using the Metropolis-Hastings algorithm with experimental data on the bolted joint using the UQLab toolbox to quantify uncertainties, in order to take advantage of the calculations performed and identify new alternatives for evaluating the parameters and quantifying the associated uncertainties in each case.

The following cases will use the same procedure, with the same conditions of estimation parameters, distribution type and interval presented in Tab. 1. However, the preload will be different, where each experimental FRF was generated with a preload of 60, 30 and 20 N.m. Fig. 6 shows the twenty Markov Chains for each thousand interactions, with their respective KDE curve, for each stiffness (vertical and torsional, respectively). The case under study, will be for preload of 60 N.m.

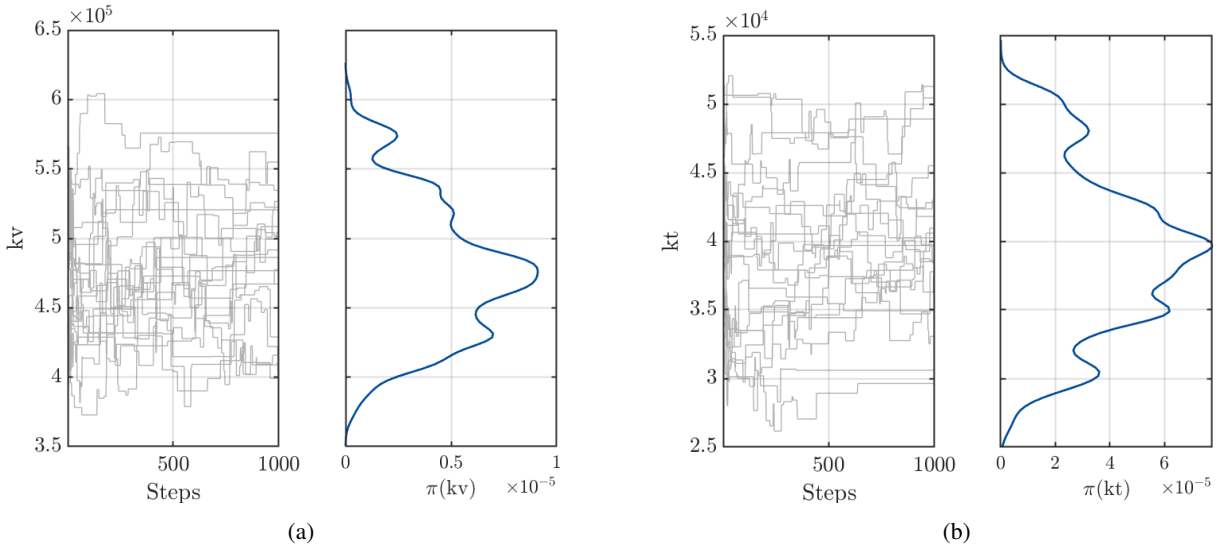

Figure 6: Trace and corresponding KDE plots during the MCMC-MH run of the estimated parameters (a) vertical stiffness and (b) torsional stiffness for preload of 60N.m

It is possible to infer from Fig. 6 that the Markov currents behave almost the same as in the previous case and that there is a peak in the densities. Table 5 presents the values of the estimated parameters, with the experimental error (from the computational analysis) and the percentage error for each parameter. The relative percentage error of the torsional stiffness parameter (k_t) decreases to less than half, as does the vertical stiffness (k_v) compared to the previous case. And this small error contributes to a good fit to the curve parameters estimated in the experimental FRF, which conditions us to understand that this estimate was correct, as shown in Figure 6. Also evaluating the correlation matrix between the estimated parameters (Tab. 5), it can be understood that they correlate at 17%, which means that the dependence between them is greater than in the previous case.

Table 4: Nominal value, expected mean, the experimental error, and the relative percent error for the parameters for preload of 60N.m.

γ_{ref}	γ_{est}	σ_{error}	**Error%**
$4.9800\ 10^5$	$4.7793\ 10^5$	$9.5862\ 10^{-8}$	4.03%
$4.1233\ 10^4$	$3.922\ 10^4$	$9.5862\ 10^{-8}$	4.86%

Table 5: The correlation matrix of the parameters for 60 N.m preload.

	(k_v)	(k_t)
(k_v)	1	0.17
(k_t)	0.17	1

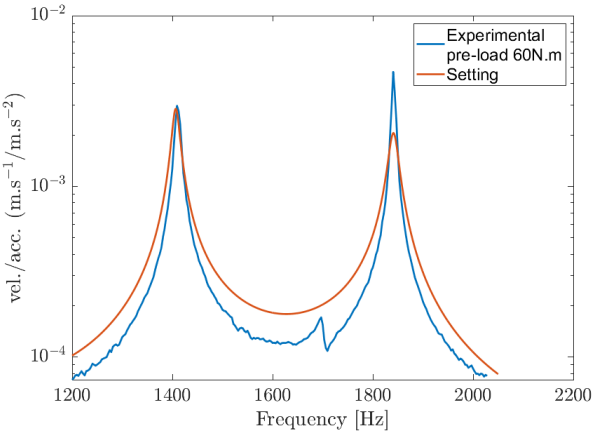

Figure 7: FRFs of the estimated parameters for each experimental data and the experimental data of the bolted joint for pre-load of 60N.m.

Repeating the process for preload of 30N.m. Fig. 8 shows the twenty Markov Chains for each thousand interactions, with their respective KDE curve, for vertical and torsional stiffness, respectively.

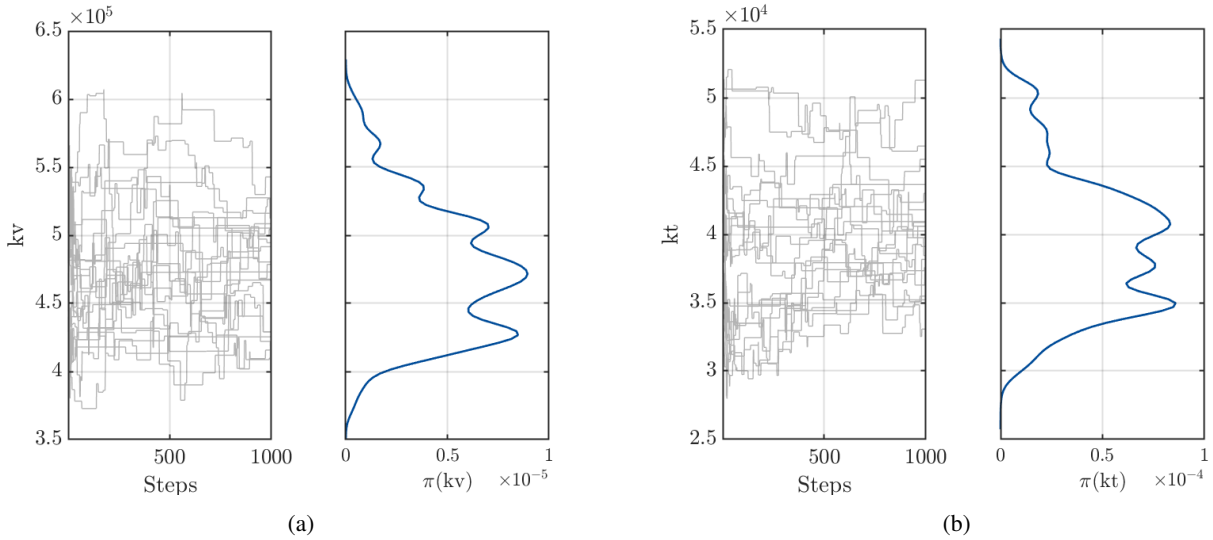

Figure 8: Trace and corresponding KDE plots during the MCMC-MH run of the estimated parameters (a) vertical stiffness and (b) torsional stiffness for preload of 60N.m

Table 6: Nominal value, expected mean, the experimental error, and the relative percent error for the parameters for preload of 30N.m.

γ_{ref}	γ_{est}	σ_{error}	**Error%**
$4.9800\ 10^5$	$4.7534\ 10^5$	$9.3361\ 10^{-8}$	4.55%
$4.1233\ 10^4$	$3.9451\ 10^4$	$9.3361\ 10^{-8}$	4.32%

Table 7: The correlation matrix of the parameters for 30 N.m. preload.

	(k_v)	(k_t)
(k_v)	1	0.22
(k_t)	0.22	1

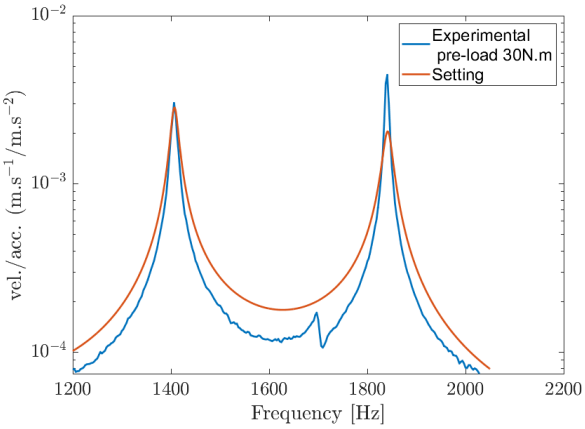

Figure 9: FRFs of the estimated parameters for each experimental data and the experimental data of the bolted joint for pre-load of 30N.m.

Figure 10 shows the behavior of the Markov chains that present the similar behavior of the previous and already expected cases; it can be seen that the densities present a peak in the estimated value. When the estimated values are evaluated with the reference value (as shown in Table 1), it can be seen that the relative percentage errors for both parameters are less than 5%, i.e., with this FRF is within the expected and can be used to calibrate the system. When looking at the correlation between the stiffnesses (Table 8), there is a correlation of 22%, higher than the previous cases.

For the last case, the preloading of 20N.m, the same method was followed to estimate the vertical stiffness and torsional stiffness parameters, with the same initial information (Table 1).

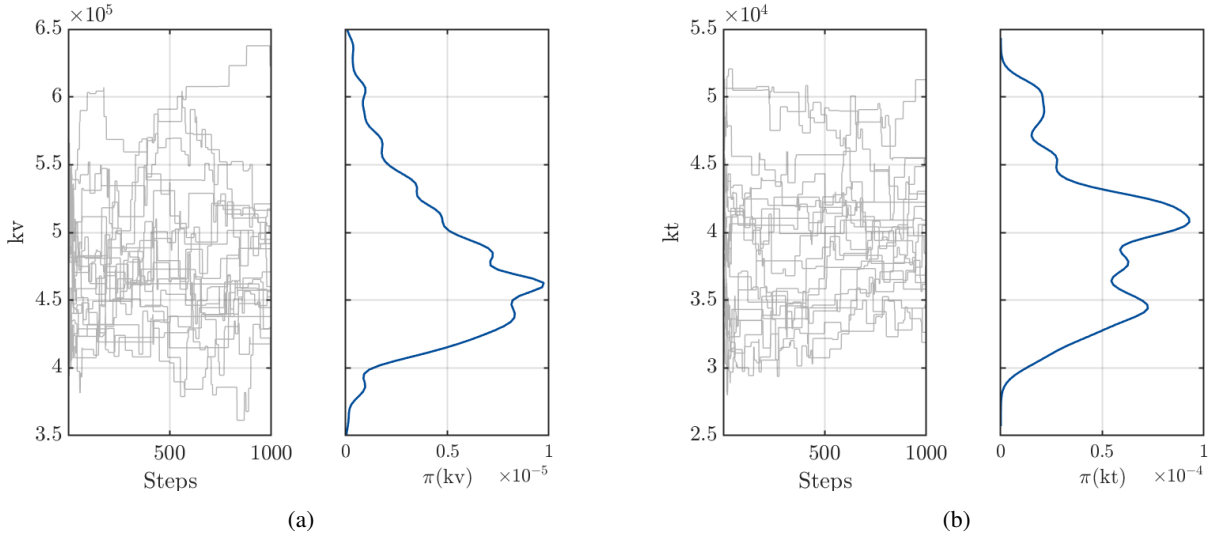

Figure 10: Trace and corresponding KDE plots during the MCMC-MH run of the estimated parameters (a) vertical stiffness and (b) torsional stiffness for preload of 20N.m

As in the previous cases, Figure 10 shows the twenty Markov chains behave as expected, where the KDE curve shows the probability of the vertical stiffness and torsional stiffness parameters for the 20N.m preload.

Table 8: Nominal value, expected mean, the experimental error, and the relative percent error for the parameters for preload of 20N.m.

γ_{ref}	γ_{est}	σ_{error}	**Error%**
$4.9800\ 10^5$	$4.7785\ 10^5$	$9.0803\ 10^{-8}$	4.04%
$4.1233\ 10^4$	$3.9315\ 10^4$	$9.0803\ 10^{-8}$	4.65%

Table 9: The correlation matrix of the parameters for 20 N.m. preload.

	(k_v)	(k_t)
(k_v)	1	0.41
(k_t)	0.41	1

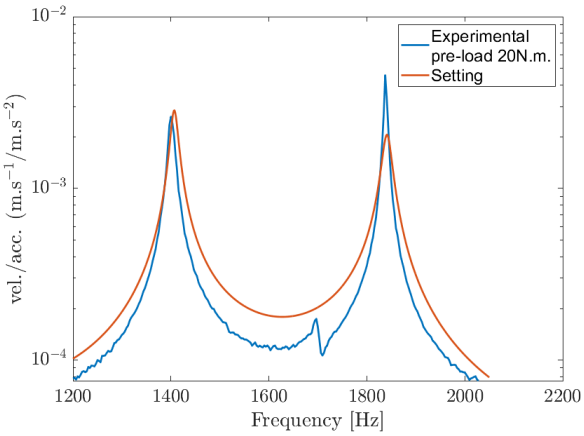

Figure 11: FRFs of the estimated parameters for each experimental data and the experimental data of the bolted joint for pre-load of 20N.m.

Figure 11 shows the estimated FRFs for data along with the experimental FRF, FRF with inferred parameters, and the probability envelope. It can be seen that the estimation was also satisfactory, because just like the previous analysis, the RMS lies within the probability envelope. Regarding the relative errors for each parameter, it can be seen that both k_v and k_t are values less than 5%. It is noted that the experimental fit was satisfactory, because they (red line) are almost coincident. The same case was observed as in the previous analysis, that the higher the frequency the further apart the peaks are, but this discrepancy is not significant. Regarding the correlation matrix, it can be seen that in this case the correlation is more expressive, 41%. After the estimations, we chose to graph the preloads and for the vertical and torsional stiffness parameters, respectively, as can be seen in Figures 12(a) and (b).

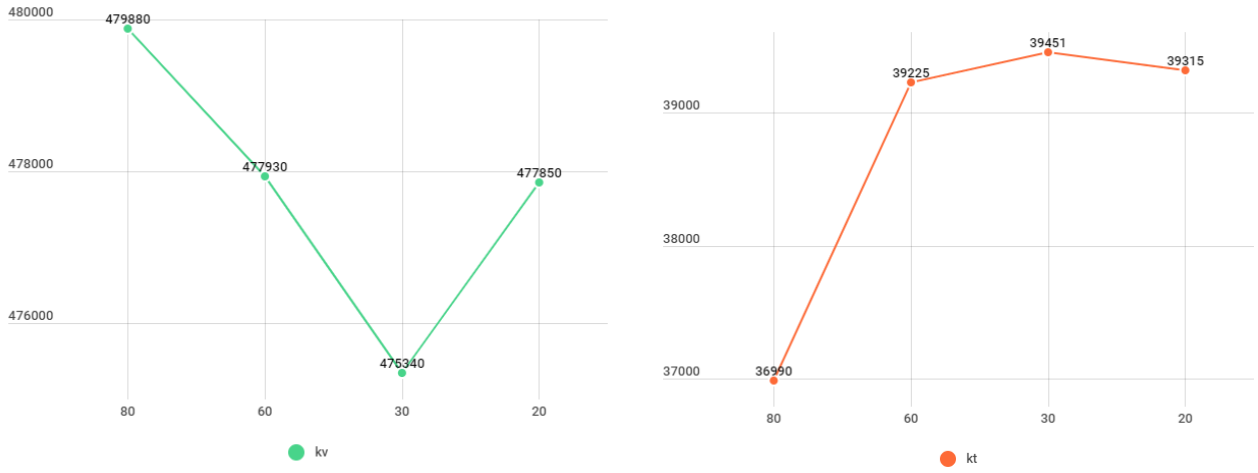

(a) (b)

Figure 12: Preloads and the respective estimated parameter (a) vertical stiffness and (b) torsional stiffness.

Figure 12(a) shows that the vertical stiffness parameter has a decreasing value as the preload decreases, but when it reaches the value of 20N.m there is a slight increase, which can be explained by the stresses between the bolt and the plates. When it comes to the other estimated parameter (Fig. 12), there is an inverse relationship between preloading and torsional stiffness. With this small difference, it can be seen that there is a relationship between preloading and the estimated parameters. With this study, one can develop a Digital Twin that relates these parameters in order to predict the behavior of the bolted joint.

CONCLUSIONS

This work was the beginning of an extensive study in Bayesian inference in continuous system, which has being explored in the literature. With the advance of Industry 4.0, the use of Digital Twin is being widely used as a means of improving the performance of physical systems by leveraging computational techniques. Interest in the Digital Twin has increased in recent years, both in academia and in industry, due to the proposition of building a numerical model with high fidelity to the real system. A Digital Twin environment allows for rapid testing and real-time decisions made through accurate analyses. In all cases, Bayesian inference proved satisfactory when searching for results correlating probability density functions using probabilistic models. We applied the MCMC probabilistic methodology using the Metropolis-Hastings algorithm to the experimental data using the UQLab Toolbox for Uncertainty Quantification and leveraged the calculations performed to provide a parameter estimate of each uncertainty. It can be seen that there is a correlation between preloading and stiffness, and this was demonstrated by the tests. Thus, various methodologies for governing Bayesian inference in parameter estimation have been obtained for both numerical and experimental models.

REFERENCES

Alfattani, R., 2020. ”Modeling and simulation of the static structural response and lift-off of a preloaded bolted joint on a flange.” Proceedings, Vol. 63, No. 1, p. 10. ISSN 2504-3900. doi:10.3390/proceedings2020063010.

Castello, D., Kaipio, J. ”Modeling errors due to Timoshenko approximation in damage identification”. International Journal Numerical Methods Eng. 2019; 120: 1148– 1162. https://doi.org/10.1002/nme.6175

Doyle, J.F., 1997. ”Wave propagation in structures: spectral analysis using fast discrete Fourier transforms.” Mechanical Engineering. Springer-Verlag New York, Inc, New York, 2nd ed.

Kim, J., Yoon, J., and Kang, B., 2007a. ”Finite element analysis and modeling of structures with bolted joints.” Applied Mathematical Modeling, Vol. 31, pp. 895-911.

Knight, N., Phillips, D., and Raju, I., 2008. ”Simulation of the structural response of a preloaded bolted joint.” In Proceedings of the 49th AIAA/ASME/ASCE/AHS/ASC Structures, Structural Dynamics, and Materials Conference, Schaumburg, IL, USA. pp. 1-20. doi:10.2514/6.2008-1842.

Lataniotis, C.; Marelli, S.; Sudret, B. ”Uncertainty quantification in the cloud with UQCloud”. In: 4th International Conference on Uncertainty Quantification in Computational Sciences and Engineering (UNCECOMP 2021). ETH Zurich, Chair of Risk, Safety and Uncertainty Quantification, 2021. p. U 18990.

Lee, U. and Lee, C., 2009. ”Spectral element modeling for extended Timoshenko beams”. Journal of Sound and Vibration. 319. 993-1002. 10.1016/j.jsv.2008.06.048.

Lee, U., 2001. “Dynamic characterization of the joints in a beam structure by using spectral element method”. Shock and Vibration, Vol. 8, No. 6, pp. 357–366.

Lee, U.. ”Spectral Element Method in Structural Dynamics”. 1st ed. Wiley, 2009. Web. 25 Sept. 2021.

Machado, M. R., Appert, A. and Khalij, L., 2019. “Spectral formulated modelling of an electrodynamic shaker”. Mechanical, Research Communication, Vol. 97, pp. 70–78.

Narayanan, G. and Beskos, D., 1978. ”Use of dynamic influence coefficients in forced vibration problems with the aid of Fast Fourier Transform”. Computers & Structures, Vol. 9, No. 2, pp. 145–150.

Oldfield, M., Ouyang, H., Mottershead, J.E., and Kyprianou, A., 2003. ”Modeling and simulation of bolted joints under harmonic excitation.” Materials Science Forum, Vol. 440-441, pp. 421-428. ISSN 16629752.

Ritto, T.G. and Castello, D., 2016. ”Quantificação de incertezas e estimação de parâmetros em dinâmica estrutural: uma introdução a partir de exemplos computacionais,”

Soo Kim, T. and Kuwamura, H., 2007. ”Finite element modeling of bolted connections in thin-walled stainless steel plates under static shear.” Thin-Walled Structures, Vol. 45, No. 4, pp. 407-421. ISSN 02638231.

Teloli, R. de O., Butaud, P., Chevallier, G., and da Silva, S., 2021, ”Dataset of experimental measurements for the Orion beam structure.” Data in Brief, Vol. 39, pp. 107627, 2021.

Teloli, R. de O., Butaud, P., Chevallier, G., and da Silva, S., 2022, ”Good practices for designing and experimental testing of dynamically excited jointed structures: the Orion beam,” Mechanical Systems and Signal Processing, vol. 163, no. June 2021, pp. 108172, 2022.

Wagg, D. J., Worden, K., Barthorpe, R. J., and Gardner, P., 2020. ”Digital Twins: State-of-the-Art and Future Directions for Modeling and Simulation in Engineering Dynamics Applications.” ASME. ASME J. Risk Uncertainty Part B. September 2020; 6(3): 030901. https://doi.org/10.1115/1.4046739

Zeng, G. and Zhao, D., 2011. ”Simulation and experiment of the dynamics of a bolted flange structure with bolted joint”. Advanced Materials Research, Vol. 335-336, pp. 543-546. ISSN 10226680.

RESPONSIBILITY NOTICE

The authors are the only responsible for the printed material included in this paper.